Conditional moment closure of mixing and reaction in turbulent nonpremixed combustion

By Nigel S. A. Smith[1]

1. Motivation

Nonpremixed combustion is the process whereby fuel and oxidizer species, which are each nonflammable in isolation, concurrently mix to form a flammable mixture, and chemically react in the flammable mixture. In cases of practical industrial interest, the bulk of nonpremixed combustion occurs in a turbulent mixing regime where enhanced mass transfer rates allow the maximum power density to be achieved in any given thermochemical device.

Conventional moment closure techniques are inapplicable in modeling turbulent combustion because of the nonlinear dependence of chemical reactions upon small scale fluctuations in species concentrations and temperature. More sophisticated closures are required so as to model turbulent nonpremixed combustion systems of practical interest, such as in gas turbine combustors and diesel engines.

A number of sophisticated models can be found in the literature, notably the laminar flamelet method (see Peters 1984), and the joint probability density function method (see Pope 1985). Some of the issues surrounding the latter method were investigated in a recent study at the Center for Turbulence Research (see Frolov *et al.* 1996), while others have investigated the former method (see Mell *et al.* 1994).

Another model of substantial merit is the conditional moment closure (CMC) method, which was proposed independently by Klimenko (1990) and Bilger (1993). This method has been successfully compared with turbulent jet flame experiments (Smith *et al.* 1995, Smith 1994), isothermal reacting mixing layers in an atmospheric wind tunnel (Li & Bilger 1993), isothermal direct numerical simulations (Mell *et al.* 1993), and in reacting DNS with heat release and complex chemistry (Smith 1995).

The results of the most recent DNS study incorporating realistic chemistry in a direct numerical simulation indicated a sensitivity of the method to the choice of chemical mechanism used to describe the thermochemical system. The choice of mechanism was found to have an impact on the accuracy of the chemical closure itself.

Work carried out at the CTR, in the six months following Smith (1995), has been aimed at improving the mixing submodel as well as understanding the deficiencies in the chemical closure for in a generic combusting chemical system.

1 Present address: Aeronautical & Maritime Research Lab., Australia

1.1 Conditional moment closure method

The classical difficulty faced in modeling turbulent nonpremixed combustion is that of closing the averaged equations for chemically reactive species. The instantaneous equation for the evolution of the mass fraction Y_α of a reactive species α is the following,

$$\frac{\partial}{\partial t}(\rho Y_\alpha) + \frac{\partial}{\partial x_i}(\rho u_i Y_\alpha) = \frac{\partial}{\partial x_j}(\rho D_\alpha \frac{\partial Y_\alpha}{\partial x_j}) + \rho \dot{w}_\alpha \tag{1}$$

where $\dot{w}_\alpha$ is the net chemical production rate of the species α, and D_α is the corresponding molecular diffusivity where a simplified Fickian approximation has been made to model molecular transport. Applying a traditional averaging scheme, such as density-weighted (Favre) unconditional ensemble averaging, yields the following,

$$\frac{\partial}{\partial t}(\bar{\rho}\tilde{Y}_\alpha) + \frac{\partial}{\partial x_i}(\bar{\rho}\widetilde{u_i Y}_\alpha) = \frac{\partial}{\partial x_j}(\bar{\rho} D_\alpha \widetilde{\frac{\partial Y_\alpha}{\partial x_j}}) + \bar{\rho}\tilde{\dot{w}}_\alpha. \tag{2}$$

In order to close the averaged species equation, a model must be provided for the averaged source term $\tilde{\dot{w}}_\alpha$. First order closures that evaluate the instantaneous chemical rate expressions with averaged species concentrations and temperature,

$$\tilde{\dot{w}}_\alpha(Y_1, Y_2, \ldots, Y_N, T) \not\approx \dot{w}_\alpha(\tilde{Y}_1, \tilde{Y}_2, \ldots, \tilde{Y}_N, \tilde{T}) \tag{3}$$

are known to be highly inaccurate in combustion cases of practical interest. The chemical reactions encountered in combustion processes are highly nonlinear, and thus small perturbations in the input parameters can cause very large changes in the computed reaction rate.

Under the Conditional Moment Closure (CMC) method, the level of perturbations from the modeled mean data is reduced by averaging the reactive species equations *conditionally* upon a conserved scalar mass fraction.

At the expense of adding an additional computational dimension to the modeling problem, conditional averaging allows chemical closure to be effected in many cases of nonpremixed turbulent combustion.

The average of a fluctuating turbulent quantity A, conditional upon the conserved scalar mixture fraction $\xi(x_i, t)$ being equal to a sample value η, is the following (see Klimenko (1990)):

$$\langle A(x_i, t) \mid \xi(x_i, t) = \eta \rangle \equiv \frac{1}{P_\eta} \int \int A(x_i, t) \delta(\xi(x_i, t) - \eta) dx_i dt \tag{4}$$

In the above definition, P_η is the probability density function of the conserved scalar at the location x_i and time t, and δ denotes the Dirac delta function. In all that follows, the full conditional averaging operator $\langle \ldots \mid \xi(x_i, t) = \eta \rangle$ will be abbreviated to $\langle \ldots \mid \eta \rangle$ for the sake of brevity.

The evolution of the conditional mean mass fraction $Q_\alpha \equiv \langle Y_\alpha \mid \eta \rangle$ of a reactive species α is governed by the following,

$$\langle \rho \mid \eta \rangle \frac{\partial Q_\alpha}{\partial t} + \langle \rho u_i \mid \eta \rangle \frac{\partial Q_\alpha}{\partial x_i} = \frac{1}{2} \langle \rho \chi \mid \eta \rangle \frac{\partial^2 Q_\alpha}{\partial \eta^2} + \langle \rho \dot{w}_\alpha \mid \eta \rangle + e_q + e_y \tag{5}$$

where the molecular diffusivities of all species are assumed uniform. The residual terms, e_q and e_y, contained unclosed expressions involving the conditional means and variations from the conditional means. These terms are presumed small in the cases studied here.

The symbol χ denotes the instantaneous scalar dissipation rate and is defined (below) in terms of the mixture fraction ξ.

$$\chi \equiv 2 D_\xi (\frac{\partial \xi}{\partial x_i})^2 \tag{6}$$

In order to close the CMC scalar equation, means of determining $\langle \rho \chi \mid \eta \rangle$ and $\langle \dot{w}_\alpha \mid \eta \rangle$ are required. The conditional mean scalar dissipation rate, $\langle \rho \chi \mid \eta \rangle$, is determined from the conserved scalar PDF equation so as to ensure conservation of mass. The calculation of this quantity is discussed in a later section.

1.2 Chemical source terms

The net volumetric chemical formation rate (dimensions of $mol/(L^3 T)$) of a reactive species is most commonly described as a linear combination of Arrhenius type expressions, as given below:

$$\dot{\omega}_\alpha = \sum_{\beta=1}^{N_r} c_{\alpha,\beta} [K_\beta(T) \prod_{\gamma=1}^{N_s} Y_\gamma^{\nu_{\gamma,\beta}}]. \tag{7}$$

The net production rate of the species α is equal to the weighted sum of the production by all chemical reactions ($\beta = 1, \ldots, N_r$). The weighting factor for species α and reaction β, $c_{\alpha,\beta}$, is an integer in the case of elementary reactions and may be positive or negative or zero (no net effect).

Each individual reaction is governed by the law of mass action, and a so-called reaction rate "constant," K_β, as given below:

$$K_\beta(T) = \rho^{n_\beta} k_\beta(T) = (\frac{p}{R})^{n_\beta} \lambda_\beta T^{a_\beta} \exp -\theta_\beta / T. \tag{8}$$

Reaction rate constants are typically strongly nonlinear functions of temperature, T, and to a lesser extent pressure. The activation temperature is denoted by θ_β, the reaction order by n_β, and the pre-exponential coefficient by λ_β.

A Taylor series expansion in terms of temperature and the participating reactants in each reaction can easily be derived. Neglecting terms third order and higher, an expression for the conditional mean source term for a species α can be written in

terms of conditional mean species mass fractions Q_γ, as well as the first and second conditional moments of temperature and the reactant mass fractions.

$$\langle \dot{w}_\alpha \mid \eta \rangle \approx \sum_{\beta=1}^{N_r} c_{\alpha,\beta} K_\beta(\langle T \mid \eta \rangle) r_\beta \prod_{\gamma=1}^{N_s} Q_\gamma^{\nu_{\gamma,\beta}} \tag{9}$$

The modifying function r_β from the above equation is defined as follows for a bimolecular reaction with reactant species Y_1 and Y_2,

$$r_\beta = 1 + B_\beta \frac{\langle (T')^2 \mid \eta \rangle}{\langle T \mid \eta \rangle^2} (1 + \frac{\sigma_{1,2}}{Q_1 Q_2}) + A_\beta (\frac{\sigma_{1,T}}{Q_1 \langle T \mid \eta \rangle} + \frac{\sigma_{2,T}}{Q_2 \langle T \mid \eta \rangle}) \tag{10}$$

where,

$$B_\beta = \frac{1}{2}((a_\beta + \theta_\beta / \langle T \mid \eta \rangle)^2 - a_\beta - 2\theta_\beta / \langle T \mid \eta \rangle) \tag{11}$$

and

$$A_\beta = a_\beta + \theta_\beta / \langle T \mid \eta \rangle \tag{12}$$

In the majority of previous CMC modeling efforts, the function r_β has been assumed to equal unity. It is, however, clear that in instances where the activation temperature θ_β, or the temperature exponent a_β are large, chemical closure is sensitive to even small levels of conditional variance.

2. Objectives

The objective of the most recent work has been to evaluate the level of departure of the modifying function r_β away from unity, over a range of reaction types within a turbulent nonpremixed combustion system. Of particular interest is the behavior of the modifying function for the rate controlling reaction for the thermal production of nitric oxide (NO) given below:

$$N_2 + O \rightarrow NO + N.$$

The reaction above has a very high activation temperature and would seem susceptible to errors which might arise from assuming a unit modifying function. This is of particular significance to existing comparisons between experiment and simple first-order closure CMC calculations (see Smith *et al.* 1995) in turbulent jet flames of hydrogen. In those cases, the model appears to consistently overpredict NO levels while more or less accurately predicting the major reaction products.

In order to evaluate the advantage that might be gained by allowing for non-unity modifying functions, direct numerical simulations of weakly turbulent nonpremixed combustion of methane in air were performed. The chemical mechanism employed included NO formation through prompt and thermal reaction pathways, in addition to major species production.

The simulation conditions were arranged as much as possible to make best use of the limited number of grid points in the domain in collecting a statistical sample. The simulation was organized such that a substantial portion of the domain could be treated as statistically similar.

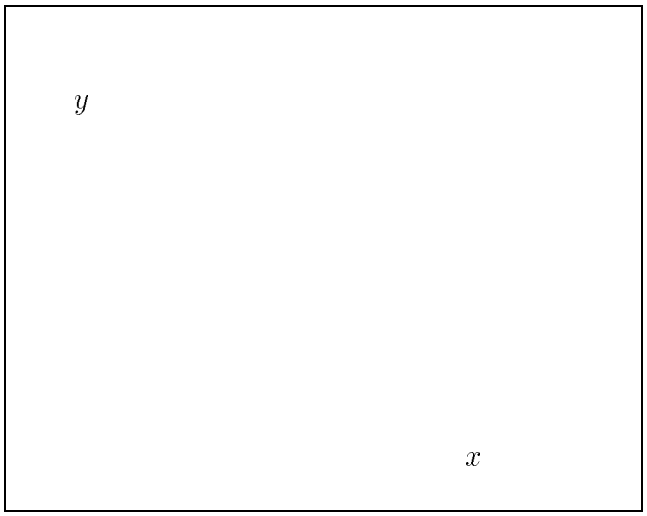

FIGURE 1. Initial distribution of the conserved scalar. White regions denote $\xi = 1$ while black regions denote $\xi = 0$. Initial conserved scalar unmixedness $\Omega = 0.64$.

2.1 Simulation conditions

The DNS code that was used is little changed from that described previously (see Smith 1995, Ruetsch & Broadwell 1995). The code features a the high-order compact finite differencing scheme, as described by Lele (1992), for spatial differencing, and the third order Runge-Kutta timestepping algorithm of Wray. The Navier-Stokes characteristic boundary conditions described by Poinsot and Lele (1992) are also included.

All simulations performed to date have been two dimensional with sizes ranging up to 257^2. It is desirable to perform three dimensional simulations of the same nature, but as yet computational resources have been insufficient to allow a reasonable Reynolds number in the calculation while carrying realistic chemistry.

2.1.1 Chemical reaction mechanism

A novel eight step reduced chemical mechanism for methane combustion (Frolov 1996) has been devised which allows substantial savings in resolution requirements over more orthodox mechanisms, while purporting to provide reasonable agreement with experiment. The mechanism consists of global steps which do not make explicit use of any radical species, such as hydroxyl (OH), methyl (CH_3), and so on, but instead employs tuning factors for the fuel oxidation and prompt NO_x steps. These tuning factors are incorporated into the pre-exponential coefficients in the Arrhenius expressions and make allowance for variations in local equivalence ratio, fuel species, and pressure. The tuning constants were derived by Frolov (1996) from comparison of the reduced mechanism with full mechanism calculations in counterflow laminar premixed flames.

$$CH_4 + 1.5O_2 \rightarrow CO + 2H_2O \qquad (I)$$

$$CO + H_2O \rightarrow CO_2 + H_2 \qquad (IIf)$$

$$CO_2 + H_2 \rightarrow CO + H_2O \qquad (IIb)$$

$$2H_2 + O_2 \rightarrow 2H_2O \qquad (III)$$

$$2CO + O_2 \rightarrow 2CO_2 \qquad (IV)$$

$$CH_4 + O_2 + N_2 \rightarrow CH_4 + 2NO \qquad (V)$$

$$N_2 + O_2 \rightarrow 2NO \qquad (VIf)$$

$$NO + NO \rightarrow N_2 + O_2 \qquad (VIb)$$

The Arrhenius rate constants corresponding to the above reaction steps are given below where λ_β, a_β and E_β denote the pre-exponential factor, temperature index, and activation energy for reaction number β, and p is the local pressure in bar.

No.	$\lambda_\beta(mol, L, s)$	a_β	$E_i(kcal/mol)$
I	A_1/p	0.0	50.0
IIf	$1.0 \times 10^{12}/p$	0.0	41.5
IIb	$3.1 \times 10^{13}/p$	0.0	49.1
III	$7.0 \times 10^{13}/p^2$	0.0	21.0
IV	$8.5 \times 10^{12}/p^2$	0.0	21.0
V	A_5/p^2	0.0	50.0
VIf	1.7×10^{17}	-0.5	136.0
VIb	4.1×10^{15}	-0.5	93.3

The pre-exponential factors for reactions I and V are functions of the local equivalence ratio β. Frolov (1996) determined the appropriate values of λ_1 and λ_5 at a range of equivalence ratios from $\beta = 0.67$ up to $\beta = 1.54$. The pre-exponential factors vary nonlinearly over the range such that the lean limit values are orders of magnitude greater than the rich limit values. The values under stoichiometric conditions for each is $\lambda_1 = 2.57 \times 10^{15} L/(mol \cdot s)$ and $\lambda_5 = 7.03 \times 10^{13} L^2/(mol^2 s)$. At the suggestion of Frolov (1996), linear interpolation between the known values for λ_1 and λ_5 was used to determine values for intermediate mixing states.

2.1.2 Domain initialization

The turbulent field was initialized using an incompressible phase scrambled kinetic energy spectrum for the velocity components and a conserved scalar. The initialized conserved scalar field can be seen Fig. 1, where black regions denote pure oxidizer zones and white regions denote pure fuel zones. Scalar *normalized unmixedness* can be defined as:

$$\Omega \equiv \frac{\langle \xi^2 \rangle}{\langle \xi \rangle (1 - \langle \xi \rangle),} \qquad (13)$$

which can be seen to be a normalized measure of the fluctuation level. Unmixedness varies between zero, where the scalar field is homogeneous, and unity where only

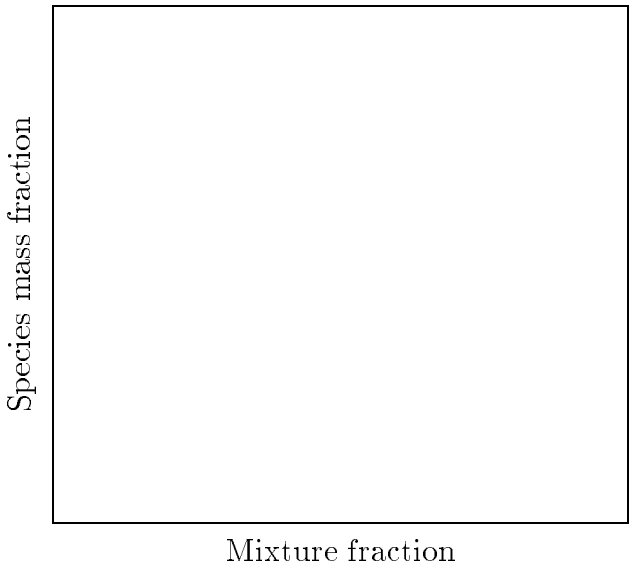

FIGURE 2. Adiabatic equilibrium species mass fraction profiles in mixture fraction space. Symbol key : $+$ - O_2, $\times$ - CO, $\circ$ - CO_2, $\triangle$ - H_2O.

pure fuel and pure oxidizer zones exist with no mixing at all. The initial conserved scalar fields used here had initial unmixednesses of $\Omega \approx 0.8$ in all cases.

Reactive species' mass fractions and internal energy were mapped onto the conserved scalar field using adiabatic chemical equilibrium relationships between mixture fraction (conserved scalar) and the reactive scalars. The adiabatic equilibrium reactive scalar mass fraction profiles are plotted versus conserved scalar mixture fraction in Fig. 2.

Note that the chemical conditions in the richest permissible mixture corresponded to a state with an equivalence ratio of approximately three. This mixture fraction is beyond the rich flammability limit of methane-air mixtures at standard temperature and pressure. Of all the species present in the simulation, only nitric oxide (NO) was initialized as being zero at all mixture fractions.

By initializing the simulation using the method described above, the flame zones were effectively ignited simultaneously, albeit artificially, prior to run time. This was done to avoid a potentially long transient period where (presumably) triple flames would propagate along the unburnt flammable ribbons between the fuel and oxidizer pockets away from the ignition points.

In order to avoid the establishment of intense pressure waves as a result of mapping flame zone temperatures onto an initial cold flow field, the local densities were adjusted everywhere to maintain a uniform initial pressure field. The existence of large density gradients after initialization caused a short period where the flow field reorganized to preserve continuity. It is difficult to draw a parallel in behavior between the decay of turbulent motions in the reacting case and the well known trends in inert grid turbulence. The former case is subject to dilatation, variable viscosity, and baroclinic torque effects that are absent in the latter.

Unfortunately, it was further found that it was not possible to perform simulations

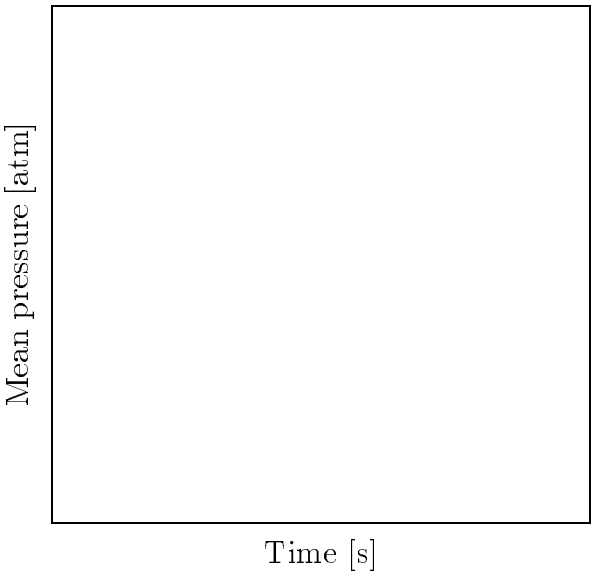

FIGURE 3. Simulated and modeled mean pressure as a function of time. Symbol key : + - DNS, × - CMC model

with a combination of periodic boundary conditions and the initialization technique described above. No satisfactory explanation for this restriction has been found. It was found, however, that the calculation could proceed without hindrance if the domain was instead bounded by adiabatic slip walls encompassing a small filter zone with initially damped wall-normal velocity.

Under the simulation conditions described above, the flow and mixing fields on a central portion of the grid (210^2) were found to be statistically homogeneous. All of these points were then used in each of the statistical samples taken periodically throughout the temporal evolution of the simulation. With the passage of time, turbulent motions caused parcels of fuel and oxidizer to be convected into close proximity while molecular diffusion fed the reaction zones present at the fuel/oxidizer interfaces.

2.2 Modeling method

Conditional moment closure model calculations were made for the same conditions as were present in the simulation. These calculations were made with unit chemical modifying functions r_β (see Eq. 10).

The spatially degenerate CMC and PDF equations corresponding to statistically isotropic conditions with uniform molecular diffusivities are given below,

$$\langle \rho \mid \eta \rangle \frac{\partial Q_\alpha}{\partial t} = \frac{1}{2} \langle \rho\chi \mid \eta \rangle \frac{\partial^2 Q_\alpha}{\partial \eta^2} + \langle \rho \dot{w}_\alpha \mid \eta \rangle \tag{14}$$

$$\frac{\partial}{\partial t}(\langle \rho \mid \eta \rangle P_\eta) = -\frac{1}{2} \frac{\partial^2}{\partial \eta^2}(\langle \rho\chi \mid \eta \rangle P_\eta) \tag{15}$$

where the conditional averages are taken over the entire domain and residual terms have been neglected.

The CMC equation (Eq. 5) was solved with the conditional mean scalar dissipation rate profile being given by the PDF equation in the following manner:

$$\langle \rho\chi \mid \eta \rangle = \frac{-2}{P_\eta} \int \int \frac{\partial}{\partial t}(\langle \rho \mid \eta' \rangle P_{\eta'}) d\eta' d\eta' \tag{16}$$

In this study it is possible to use PDF information from the simulation to determine the conditional mean scalar dissipation rate, but in practice this information will not typically be available to the modeler.

The form of the density-weighted PDF, $(\langle \rho \mid \eta \rangle P_\eta / \langle \rho \rangle)$, was assumed to be a Beta function. This assumption reduces the number of degrees of freedom in the PDF to two, namely specification of the conserved scalar mean and variance. The conditional mean density-weighted scalar dissipation rate was calculated using the time history of conserved scalar density-weighted mean and variance from the simulation, and the Beta function assumed form.

Beta functions have the useful characteristic of being able to change in gross shape, according to changes in variance. Thus where the variance is high, a beta function will have singularities at the fully mixed and fully unmixed states. Where the variance is low, the beta function form allows for the possibility of a singularity at only one of the end mixing states (depending on the value of the mean). For very low variance the beta function forms a mono-modal Gaussian-like distribution about the mean.

The effectiveness of the Beta function as an assumed form PDF has been discussed by Girimaji (1991) in relation to passive scalar mixing in isothermal isotropic turbulence.

3. Results

Over the course of the simulation, the Favre averaged mixture fraction unmixedness (see Eq. 13) decreased from near 0.65 down to 0.093. In this same period the simulated mean pressure rose from an initial pressure of one atmosphere to a final value of nearly two atmospheres. Around 56% of the available CO and 42% of the available CH_4 fuel species were consumed during the simulated burn. The total amount of CO_2 mass present increased by 138%, while the total mass of H_2O increased by 155%. Slightly more than 60 ppm of NO (by mass) was produced from an initial zero level over the course of the burn.

The effectiveness of the CMC model in predicting the mean simulated trends can be gauged from Figs. 3 & 4. It is evident that the CMC model consistently overpredicts the mean pressure during the course of the burn to the point where it is in excess by 10% at the end. The model also tends to overpredict NO mass fraction levels, but to a greater degree. The NO mass fraction discrepancy is on the order of 150% towards the end of the burn.

Figure 5 is provides a comparison of the simulated and predicted conditional mean temperature profiles at two different stages of the burn. In the figure, the temperature has been normalized by the adiabatic equilibrium temperature of a stoichiometric mixture at one atmosphere (2216 K). At the earlier time, some 0.28

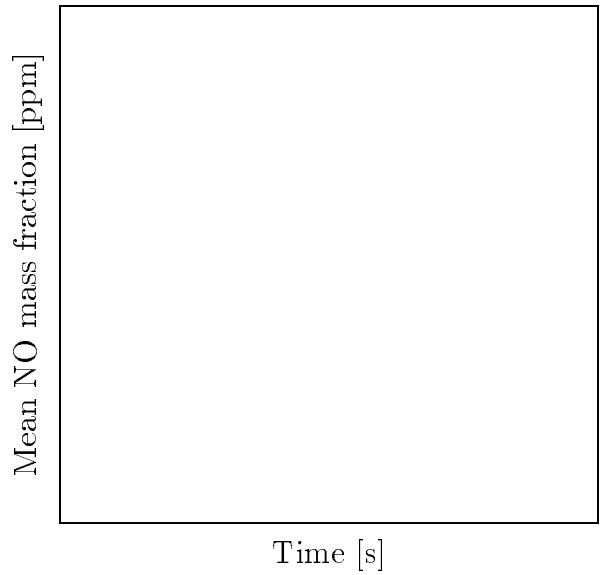

FIGURE 4. Simulated and modeled mean NO mass fraction as a function of time. Symbol key : $+$ - DNS, $\times$ - CMC model

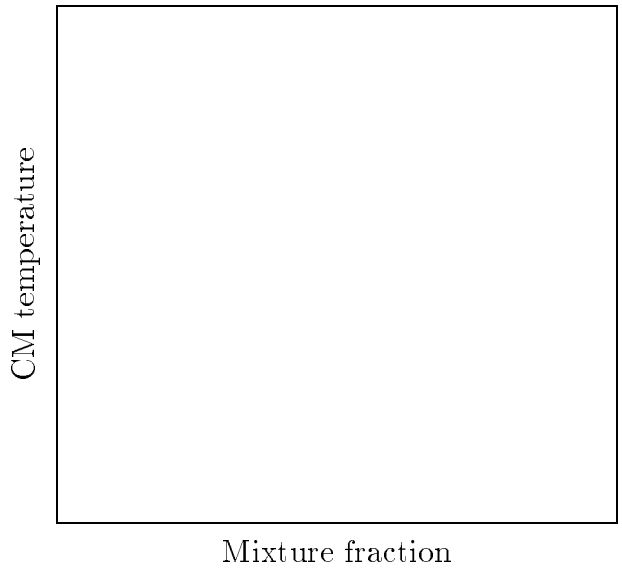

FIGURE 5. Simulated and modeled conditional mean (normalized) temperature as a function of mixture fraction for two different times. Symbol key : $\times$ - DNS at $0.28ms$, $+$ - DNS at $2.0ms$, $\circ$ - CMC at $0.28ms$, $\triangle$ - CMC at $2.0ms$.

milliseconds into the burn, the location of the CMC predicted peak conditional mean temperature is clearly shifted towards the rich side compared to the corresponding simulated profile. At that time, the actual values of the predicted and simulated profiles agree quite closely.

At the later time of 2 milliseconds, the rich shift in the predicted peak temperature location is much less pronounced, but still discernible. The overprediction of the peak temperature by the model at this time is consistent with the level of mean

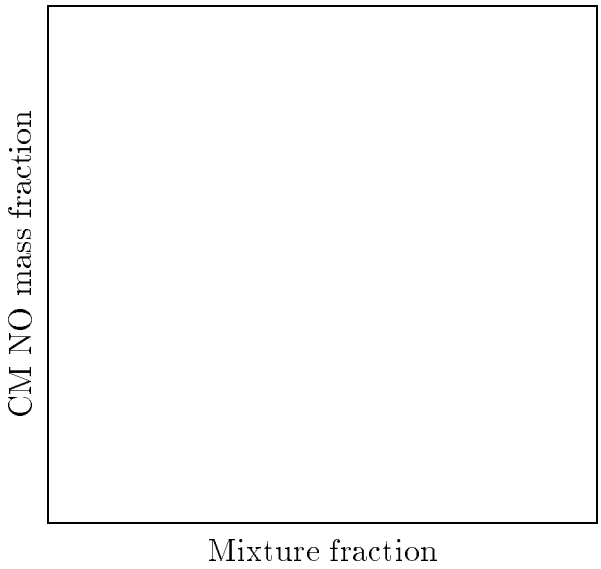

FIGURE 6. Simulated and modeled conditional mean NO mass fraction (ppm) as a function of mixture fraction for two different times. Symbol key : $\times$ - DNS at $1.2ms$, $+$ - DNS at $2.0ms$, $\circ$ - CMC at $1.2ms$, $\triangle$ - CMC at $2.0ms$.

pressure discrepancy seen in Fig. 3.

Simulated and predicted conditional mean NO mass fractions (in parts per million) are plotted for comparison in Fig. 6. The predicted profiles are substantially elevated over the corresponding simulated profiles at all times. The level of overprediction of the peak conditional mean NO mass fraction increases with time, both in relative and absolute terms. It is apparent that at the earlier time, the location of the model's peak mass fraction is shifted compared to the simulation's peak. At the later time, there is no significant shift in location between the modeled and simulated peak mass fractions.

4. Discussion

The results presented above serve to illustrate some of the current difficulties that can face CMC modelers when they seek to apply the model to problems of practical interest.

4.1 Conditional mean scalar dissipation rate

As was mentioned in section 2.2, the practical determination of conditional mean scalar dissipation rate currently relies on the assumption that the actual mixture fraction PDF conforms closely to a convenient assumed form. It is fairly clear that in the instance of isothermal mixing in isotropic turbulence, the usage of a beta function assumed form is most likely adequate (see Girimaji 1991).

However, there is a question as to whether these assumed forms, which are used in isothermal cases, remain accurate when used to embody density-weighted PDFs in cases with variable density.

The difference between the modeled and simulated conditional mean scalar dissipation rate profiles can be determined from Fig. 7. It is clear that the modeled

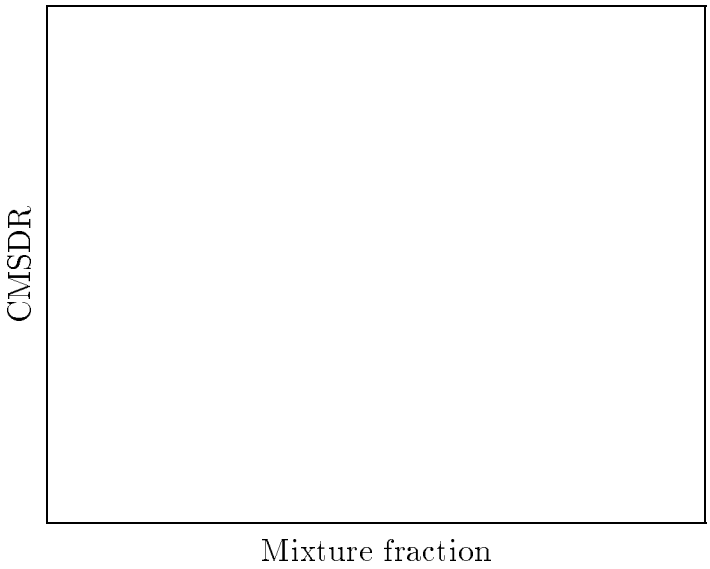

FIGURE 7. Simulated and modeled conditional mean scalar dissipation rate $\langle \chi \mid \eta \rangle$ as a function of mixture fraction for two different times. Symbol key : $\times$ - DNS at $0.28ms$, $+$ - DNS at $2.0ms$, $\circ$ - CMC at $0.28ms$, $\triangle$ - CMC at $2.0ms$.

profiles agree quite well in terms of general magnitude with the simulated profiles, at both time points.

There are however, significant differences in shape between the modeled and predicted profiles that are particularly present at early times in the burn. The modeled profiles invariably tend to approximate inverted parabolas under the range of mixture fraction variance studied here. The simulated profiles tend to have a cleft at or near the location of maximum heat release.

The existence of this departure from a simple parabolic form, is coincident with the type of unexpected lean shift seen in the simulated conditional mean temperature profiles at early times in the burn (see Fig. 5). The presence of a low region in the conditional mean scalar dissipation rate profile on the lean side of the stoichiometric mixture fraction (~ 0.367) would locally minimize the level of temperature depression below chemical equilibrium. The mixture on the rich side of stoichiometric is subject to more intense local mixing and so would tend to exhibit greater temperature depression.

A possible explanation for the asymmetric shape of the simulated conditional mean scalar dissipation rate profiles can be gleaned from a rearrangement of Eq. 15.

$$\langle \rho \mid \eta \rangle \frac{\partial P_\eta}{\partial t} + P_\eta \frac{\partial}{\partial t}(\langle \rho \mid \eta \rangle) = -\frac{1}{2}\frac{\partial^2}{\partial \eta^2}(\langle \rho\chi \mid \eta \rangle P_\eta) \tag{17}$$

Bearing in mind that conditional mean scalar dissipation rate is obtained from this equation through the double integration of both sides, then it would appear that wherever the local change in conditional mean density is particularly rapid, it could have an unusual influence on the form of $\langle \rho\chi \mid \eta \rangle$.

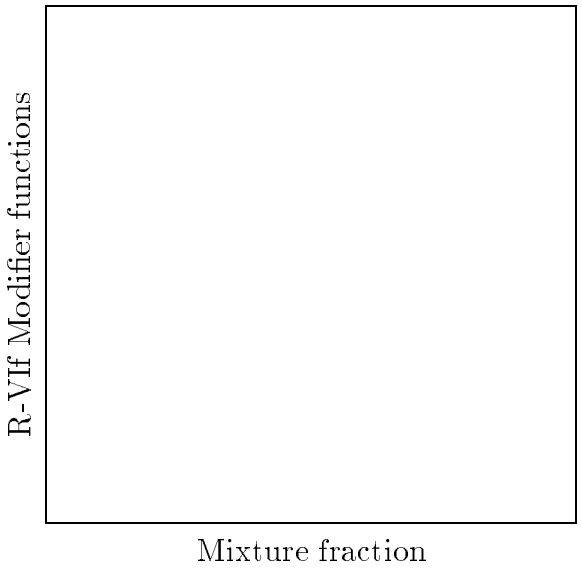

FIGURE 8. Chemical modifier functions for thermal NO formation reaction (R-VIf) determined from DNS data, $2.0ms$ into the burn. Symbol key : $+$ - r_β, $\circ$ - B_β grouping, $\triangle$ - A_β grouping.

For cases where pressure is assumed to be uniform across all mixture fractions, the conditional mean density is linked inversely to the conditional mean specific thermal energy ($\langle e \mid \eta \rangle$). An expression for the time rate of change of conditional mean density can be written as,

$$\frac{\partial \langle \rho \mid \eta \rangle}{\partial t} = \frac{1}{\langle e \mid \eta \rangle} [\int_0^1 P_{\eta'} \langle \dot{s}_e \mid \eta' \rangle d\eta' - \langle \rho \mid \eta \rangle \frac{\partial \langle e \mid \eta \rangle}{\partial t}] \tag{18}$$

where $\langle \dot{s}_e \mid \eta \rangle$ is the conditional mean chemical energy production rate. Both the chemical source term and the entire time rate of change in conditional mean thermal energy are required in any case for the solution of the full set of CMC equations.

It may be possible to employ some kind of assumed form for the *unweighted* mixture fraction PDF (P_η), and use the above pair of equations to determine $\langle \rho\chi \mid \eta \rangle$. This method is practically difficult since the energy derivative term requires $\langle \rho\chi \mid \eta \rangle$ in order to be evaluated in the first place, and thus would entail the iterative solution of an integro-differential equation. Furthermore, it is not clear that the unweighted PDF should conform to an easily parameterized assumed form such as the beta function. Such an approach risks inconsistency between the derivative of the arbitrary assumed form PDF and the computed conditional mean density derivative, which may lead to unphysical $\langle \rho\chi \mid \eta \rangle$ profiles.

4.2 Second order chemical closure

It is evident that the CMC model prediction for the rate of nitric oxide formation greatly exceeds the simulated rate. In part, this is no doubt due to the overprediction of conditional mean temperature by the CMC model. An additional $100 - 200K$ in peak conditional mean temperature in can double or triple the rate of NO formation via thermal reaction pathways.

It is instructive to also examine the chemical modifier functions r_β, A_β and B_β (see Eqs. 10-12) for the thermal NO formation reaction (R-VIf) as determined from the simulation.

The effect of neglecting second order terms in the conditional mean chemical closure can be determined from Fig. 8. The lower trace corresponds to the A_β grouping of terms, containing the conditional covariances between species and temperature. The upper trace corresponds to the B_β grouping, containing covariances between the reactant species, and the variance of temperature. The middle trace corresponds to the modifier function r_β and is equal to unity plus the sum of the other two traces.

In the reactive section of mixture fraction space around stoichiometric, the modifier function dips below the unit line by as much as $\sim 50\%$. This indicates that simple first order chemical closures, which assume a unit modifier function at all mixture fractions, will overpredict the thermal formation rate of NO by as much as 100% even given the correct conditional mean species and temperature distributions to begin with.

Fortunately, the bulk of the key reactions in typical combustion chemistry do not have as high activation energies as the thermal NO formation step and as such are not so difficult to model.

The prognosis for improved NO prediction by the CMC model is not terribly good. Short of a full second order closure scheme involving the equations for all key species variances and covariances, there is little that can be done. A partial second order closure, tracking just temperature variance or species variances alone, would not succeed since it is clear that the true r_β profile is the small difference between these two large quantities.

5. Conclusions

A study of the effectiveness of the conditional moment closure model in predicting turbulent nonpremixed combustion of methane in air has been undertaken. On the whole, the model has provided quite good agreement with the simulation for all unconditional mean species yields, with the exception of nitric oxide.

Predicted conditional mean species mass fractions and temperature were found to differ more significantly from the simulation due to small differences in the density-weighted PDF and its temporal evolution.

Large discrepancies were found in the case of nitric oxide, where higher temperatures in the model calculations and a natural tendency of the first order chemical closure to overpredict NO formation were cited as contributing factors.

Wherever practicable, future CMC model applications that seek to accurately predict NO formation should include some form of partial second order chemical closure. This should involve temperature, and the nitrogen and oxygen bearing reactant species. This is particularly desirable in combusting systems where instantaneous deviations from conditional means are expected to be large.

REFERENCES

BILGER, R. W. 1993 Conditional Moment Methods for Turbulent Reacting Flow. *Phys. Fluids.* **5,** 436-444.

FROLOV, S. M. 1996 Private communication.

FROLOV, S. M., SMITH, N. S. A., BOWMAN, C. T. 1996 Evaluation of joint probability density function models for turbulent nonpremixed combustion with complex chemistry. *Proceedings of the 1996 Summer Program*, CTR, NASA Ames/Stanford Univ., 167-186.

GIRIMAJI, S. S. 1991 Assumed Beta-pdf Model for Turbulent Mixing: Validation and Extension to Multiple Scalar Mixing. *Combust. Sci. Tech.* **78,** 177-196.

KLIMENKO, A. YU. 1990 Multicomponent Diffusion of Various Admixtures in Turbulent Flow. *Fluid Dynamics.* **25,** 327-334.

LELE, S. 1992 Compact finite difference schemes with spectral-like resolution. *J. Comp. Phys.* **103,** 16.

LI, J. D., BILGER, R. W. 1993 Measurement and Predictions of the Conditional Variance in a Turbulent Reactive-Scalar Mixing Layer. *Phys. Fluids*, **5,** 3255-3264.

MELL, W. E., NILSEN, V., KOSALY, G., RILEY, J. J. 1993 Direct Numerical Simulation Investigation of the Conditional Moment Closure Model for Nonpremixed Turbulent Reacting Flows. *Combust. Sci. Tech.*, **91,** 179-186.

MELL, W., KOSALY, G., RILEY, J. J. 1994 An Investigation of Closure Models for Nonpremixed Turbulent Reacting Flows. *Phys. Fluids*, **6,** 1331-1356.

PETERS, N. 1984 Laminar diffusion flamelet models in nonpremixed turbulent combustion. *Prog. Energy Comb. Sci.*, **10,** 319-339.

POINSOT, T., LELE, S. 1992 Boundary conditions for direct simulations of compressible viscous flows. *J. Comp. Phys.*, **101,** 104.

POPE, S. B. 1985 PDF Methods for Turbulent Flows. *Prog. Energy Combust. Sci.*, **11,** 119-192.

RUETSCH, G. R., & BROADWELL, J. E. 1995 Effects of confinement on partially premixed flames. *Annual Research Briefs - 1995*, CTR, NASA Ames/Stanford Univ., 323-333.

SMITH, N. S. A. 1994 *Development of the Conditional Moment Closure Method for Modelling Turbulent Combustion.* PhD Thesis, University of Sydney.

SMITH, N. S. A. 1995 Modeling complex chemical effects in turbulent nonpremixed combustion. *Annual Research Briefs - 1995*, CTR, NASA Ames/Stanford Univ., 301-321.

SMITH, N. S. A., BILGER R. W., CARTER C. D., BARLOW R. S., CHEN, J.-Y. 1995 A Comparison of CMC and PDF Modelling Predictions with Experimental Nitric Oxide LIF/Raman Measurements in a Turbulent H_2 Jet Flame. *Combust. Sci. Tech.*, **105,** 357-375.